ORGANIC LETTERS

2002
Vol. 4, No. 11
1895−1898

Metalloporphyrin Molecular Sieves Based on Tin(IV)porphyrin Phenolates

Gary D. Fallon, Marcia A.-P. Lee, Steven J. Langford,* and Peter J. Nichols

Department of Chemistry and Centre for Green Chemistry, Monash University, Clayton, Victoria 3800, Australia

s.langford@sci.monash.edu.au

Received March 27, 2002

ABSTRACT

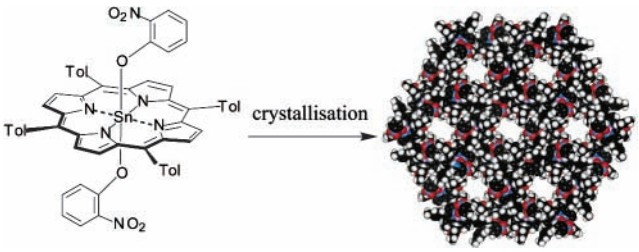

The crystal and molecular structures of two six-coordinate tin(IV)porphyrin phenolate complexes show that infinite cylindrical channels of uniform pore dimension are formed along the crystallographic *c*-direction. The underlying recognition event responsible for the porosity is an extremely tight intermeshing of the *meso*-tolyl units between layers which is a result of Sn–O···H interactions. Thermogravimetric analysis and differential scanning calorimetry have been used to characterize the sieve-like materials.

Engineered porous materials[1,2] have emerged as exciting multifunctional materials with uses as catalysts, molecular sieves, sensors, chromatographic supports, and transport devices being described.[3,4] The formation of highly ordered, infinite frameworks where the intended porous topology may occur spontaneously when suitable functionalized building blocks are engaged provides an elegant approach to the generation of sieve-like materials.[5−7] To this end, porphyrins and metalloporphyrins are interesting candidates as building blocks. Structurally, they provide a range of useful connectors through *meso* and β-pyrrolic functionalization or via the inner periphery through metalation. Their large aromatic framework and relative rigidity might well be exploited to make large cavities and channels. In this regard, there are examples of porphyrinic structures that display channel-like networks.[6,8,9] Some of these networks are characterized by the strong interaction of the porphyrin metal ion with axial ligands[6,8] while others[9] are governed by weak intermolecular interactions. Apart from the classic metal ion (Zn(II), Co(II), Mn(II))···pyridine interactive systems[6,8] in which both

(1) Chon, H., Ihm, S.-K., Uh, Y. S., Eds. *Progress in Zeolite and Microporous Materials*, Vol 105, Parts A−C; Elsevier: Amsterdam, 1997.

(2) (a) Belanger, S.; Hupp, J. T. *Angew. Chem.* **1999**, *38*, 2360−2362; *Angew. Chem., Int. Ed.* **1999**, *111*, 2222−2224. (b) Matos, J. R.; Mercuri, L. P.; Kruk, M.; Jaroniec, M. *Chem. Mater.* **2001**, *13*, 1726−1731.

(3) (a) Kuchi, V.; Oliver, A. M.; Paddon-Row, M. N.; Howe, R. F. *Chem. Commun.* **1999**, 1149−1150. (b) Eastermann, M.; McCusker, L. B.; Baerlocher, C.; Merrouche, A.; Kessler, D. *Nature* **1991**, *352*, 320−323. (c) Thomas, J. M.; Raja, R. *Chem. Commun.* **2001**, 675−687. (d) Zhao, D.; Feng, J.; Huo, Q.; Melosh, N.; Fredrickson, G. H.; Chmelka, B. F.; Stucky, G. D. *Science* **1998**, *279*, 548−552. (e) Göltner, C. G.; Henke, S.; Weibenberger, M. C.; Antonietti, M. *Angew. Chem., Int. Ed.* **1998**, *37*, 613−616.

(4) (a) Kumar, R. K.; Balasubramanian, S.; Goldberg, I. *Inorg. Chem.* **1998**, *37*, 541−552. (b) Diskin-Posner, Y.; Goldberg, I. *New J. Chem.* **2001**, *25*, 899−904. (c) Göltner, C. G.; Smarsly, B.; Berton, B.; Antonietti, M. *Chem. Mater.* **2001**, *13*, 1617−1624.

(5) (a) Abrahams, B. F.; Hoskins, B. F.; Michail, D. M.; Robson, R. *Nature* **1994**, *369*, 727−729. (b) Lu, Jianjiang; Mondal, Arunendu; Moulton, Brian; Zaworotko, Michael J. *Angew. Chem., Int. Ed.* **2001**, *40*, 2113−2116.

(6) Lin, K.-J. *Angew. Chem., Int. Ed.* **1999**, *38*, 2730−2732.

(7) (a) Ghadiri, M. R.; Granja, J. R.; Buehler, L. K. *Nature* **1994**, *369*, 301−304. (b) Benkstein, K. D.; Hupp, J. T. *Mol. Cryst. Liq. Cryst. Sci. Technol., Sect. A* **2000**, *342*, 151−158.

(8) (a) Knapp, S.; Vasudevan, J.; Emge, T. J.; Arison, B. H.; Potenza, J. A.; Schugar, H. J. *Angew. Chem., Int. Ed.* **1998**, *37*, 2368−2370. (b) Krupitsky, H.; Stein, Z.; Goldberg, I.; Strouse, C. E. *J. Incl. Phenom.* **1994**, *18*, 177.

(9) (a) Birnbaum, E. R.; Hodge, J. A.; Grinstaff, M. W.; Schaefer, W. P.; Henling, L.; Labinger, J. A.; Bercaw, J. E.; Gray, H. B. *Inorg. Chem.* **1995**, *34*, 3625−3632. (b) Cheng, R.-J.; Chen, Y.-R.; Wang, S. L.; Cheng, C. Y. *Polyhedron* **1993**, *12*, 1353−1360. (c) LeCours, S. M.; DiMagno, S. G.; Therien, M. J. *J. Am. Chem. Soc.* **1996**, *118*, 11854−11864.

10.1021/ol025935u CCC: $22.00
Published on Web 05/08/2002

potential functional groups are employed in the structural formation of the lattices, the unique nature of each of these examples suggests there is little breadth in their formation as a class. Here we report on the use of tin(IV)porphyrin phenolates as building blocks in the preparation of porous materials and suggest by way of five examples (which differ in their axial substitution) that the formation of such channels is the result of subtle cooperative effects which in essence demonstrate molecular recognition at its most fundamental level.

Tin(IV)porphyrin phenolates[10] are the stable product of the equilibrium-based condensation reaction of substituted phenols with tin(IV)porphyrin dihydroxide in an organic medium (Scheme 1). Because of the inherent simplicity of

Scheme 1. Formation of the Sn(IV)porphyrin Phenolates **1** and **2**[a]

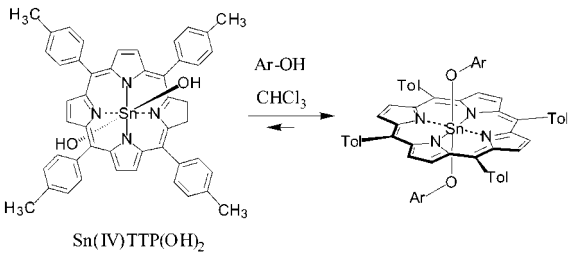

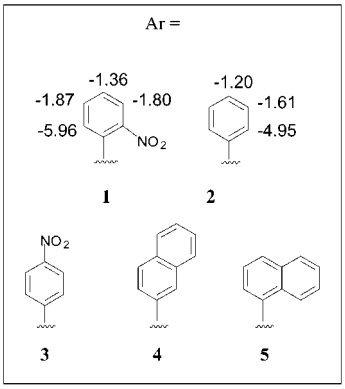

[a] As a result of the large ring current experienced by the phenol group and the subsequent large chemical shift changes (shown), this process can be easily followed by ^{1}H NMR spectroscopy. For **1** and **2**, $\Delta\delta = \delta$(complex) $-$ δ(free phenol) is shown.

axial ligation and flexibility in choice of phenolic ligand, we were interested in using Sn(IV)porphyrin phenolates to extend and complement the recent interest shown in the interplay between Sn(IV)porphyrins and carboxylic acids[11] as a convenient means of constructing functional supramolecular assemblies and arrays.[12] Condensation of Sn(IV)-TTP(OH)$_2$[13] with the desired phenol in chloroform solution at reflux for 1 h yields the porphyrin phenolate complexes **1**, **2**, **3**,[10] **4**,[14] or **5**[15] in excellent yield (>90%) after chromatography on neutral alumina.[16] Changes ($\Delta\delta$) of selected resonances in the ^{1}H NMR spectra for Sn(IV)TTP complexes of **1** and **2** are shown in Scheme 1. The very large chemical shift changes observed (> 5 ppm) are a result of the time-averaged orientation and proximity of these nuclei to the porphyrin ring current.[17]

Dark red single crystals of **1** and **2** suitable for X-ray analysis[18] were grown by vapor diffusion of hexane into chloroform solutions of **1** or **2**. The molecular structure of **1** is shown in Figure 1 , and the macromolecular structure of the arrays formed by **1** and **2** are shown in Figures 1 and 2. The metal centers of **1** and **2** are coordinated octahedrally via the four inner peripheral nitrogens of the porphyrin ligand and axially via the two phenolic oxygens (av. bond lengths: Sn−N = 2.09 Å and Sn−O = 2.07 Å for **1**, Sn−N = 2.09 Å and Sn−O = 2.06 Å for **2**). In each case the phenolate groups lie in an *anti* orientation with respect to each other. Both compounds **1** and **2** crystallize with rhombohedral symmetry (*R*3bar), giving rise to a structure constituting a graphite-like array comprising three identical, but offset, layers. Each layer constitutes a trigonal−hexagonal array of porphyrins (Figure 1B) which, based on the Sn···Sn distances in arrays of **1**, give rises to an extremely large diameter of 36.68 Å with each edge of the regular hexagon being 18.34 Å long. The distance between antipodal methyl groups within each hexagonal array of **1** is 21 Å, and allowing for the van der Waals radii of the attached hydrogens, the "free space" dimension of the channel is close to 17 Å. Each hexagon is offset to the next two in a regular fashion, giving rise to a helical path best described as 120° of every 3.5 Å (Figure

(10) Langford, S. J.; Lee, M. A.-P.; Macfarlane, K. J.; Weigold, J. A. *J. Inclusion Phenom.* **2001**, *41*, 135−139.

(11) (a) Stulz, E.; Mak, C. C.; Sanders, J. K. M.; Jeremy, K. M. *Dalton Trans.* **2001**, *5*, 604. (b) Tong, Y.; Hamilton, D. G.; Meillon, J.-C.; Sanders, J. K. M. *Org. Lett.* **1999**, *1*, 1343. (c) Kim, H.-J.; Bampos, N.; Sanders, J. K. M. *J. Am. Chem. Soc.* **1999**, *121*, 8120. (d) Maiya, B. G.; Bampos, N.; Kumar, A. A.; Feeder, N.; Sanders, J. K. M. *New J. Chem.* **2001**, *25*, 797.

(12) Giribabu, L.; Rao, T. A.; Maiya, B. G. *Inorg. Chem.* **1999**, *38*, 4971−4980.

(13) Arnold, D. P. *J. Chem. Ed.* **1988**, *65*, 1111−1112.

(14) Fallon, G. D.; M. Lee, A.-P.; Langford, S. J. *Acta Crystallogr.* **2001**, *E5*, m564−m565.

(15) Nimri,S.; Keinan, E. *J. Am. Chem. Soc.* **1999**, *121*, 8978−8982.

(16) Selected spectroscopic data. **1**: mp > 350 °C; ^{1}H NMR (300 MHz, $CDCl_3$, 300 K) δ = 1.22 (dd, J = 7.7 Hz, J = 1.4 Hz, 2H, phenol H), 2.75 (s, 12H, *meso*-ArCH_3), 5.67 (m, 4H, phenol H), 6.31 (dd, J = 7.7 Hz, J = 2.1 Hz, 2H, phenol H), 7.64 (d, J = 8.1 Hz, 8H, *meso*-ArH), 8.21 (d, J = 8.1 Hz, 8H, *meso*-ArH), 9.17 (s, 8H, β-pyrrolic H); ^{13}C NMR (75 MHz, $CDCl_3$, 300 K) δ = 21.9, 115.9, 121.5, 122.3, 123.5, 128.1, 131.2, 133.2, 135.3, 138.2, 138.6, 147.6; UV/vis ($CHCl_3$) λ_{max} (log ϵ) = 357 (4.30), 380 (4.33), 406 (4.28), 428 (5.40), 520 (3.20), 560 (3.96), 601 nm (3.80). **2**: mp > 350 °C; ^{1}H NMR (300 MHz, $CDCl_3$, 300 K) δ = 1.87 (d, J 7.3 Hz, 4H, phenol H), 2.76 (s, 12H, *meso*-ArCH_3), 5.65 (t, J = 7.3 Hz, 4H, phenol H), 5.74 (t, J = 1.2 Hz, 2H, phenol H), 7.63 (d, J = 7.8 Hz, 8H, *meso*-ArH), 8.10 (d, J = 7.8 Hz, 8H, *meso*-ArH), 9.12 (s, 8H, β-pyrrolic H); ^{13}C NMR (75 MHz, $CDCl_3$, 300 K) δ = 21.9, 116.7, 117.9, 122.0, 126.5, 127.9, 132.6, 135.2, 138.3, 138.6, 147.7; UV/vis ($CHCl_3$) λ_{max} (log ϵ) = 357 (4.30), 380 (4.33), 406 (4.28), 428 (5.40), 520 (3.20), 560 (3.96), 601 nm (3.80). We were unable to observe all ^{13}C NMR signals in $CDCl_3$ solutions of **1** or **2**.

(17) Hawley, J. C.; Bampos, N.; Sanders, J. K. M.; Abraham, R. J. *Chem. Commun.* **1998**, 661−662.

(18) Crystal data for **1**: crystal dimensions 0.22 × 0.20 × 0.14 mm, trigonal hexagonal, space group *R*3bar, a = 36.6819(3) Å, c = 10.4431(3) Å, V = 12169.2(4) Å^3, Z = 9, Final R_1 = 0.033, $wR_2(F^2)$ = 0.083, GOF = 1.11. **2**: crystal dimensions 0.38 × 0.18 × 0.14 mm, trigonal, space group *R*3bar, a = 36.7789(3) Å, c = 9.4742(3) Å, V = 11098.7(3) Å^3, Z = 9, Final R_1 = 0.024, $wR_2(F^2)$ = 0.037, GOF = 1.05. Crystallographic data (excluding structure factors) for **1** and **2** have been deposited with the Cambridge Crystallographic Data Centre as supplementary publications nos. CCDC-174917 (**1**) and CCDC-174918 (**2**). Copies of the data can be obtained free of charge on application to CCDC, 12 Union Road, Cambridge CB21EZ, UK (fax: (+44)1223-336-033. E-mail: deposit@ccdc.cam.ac.uk).

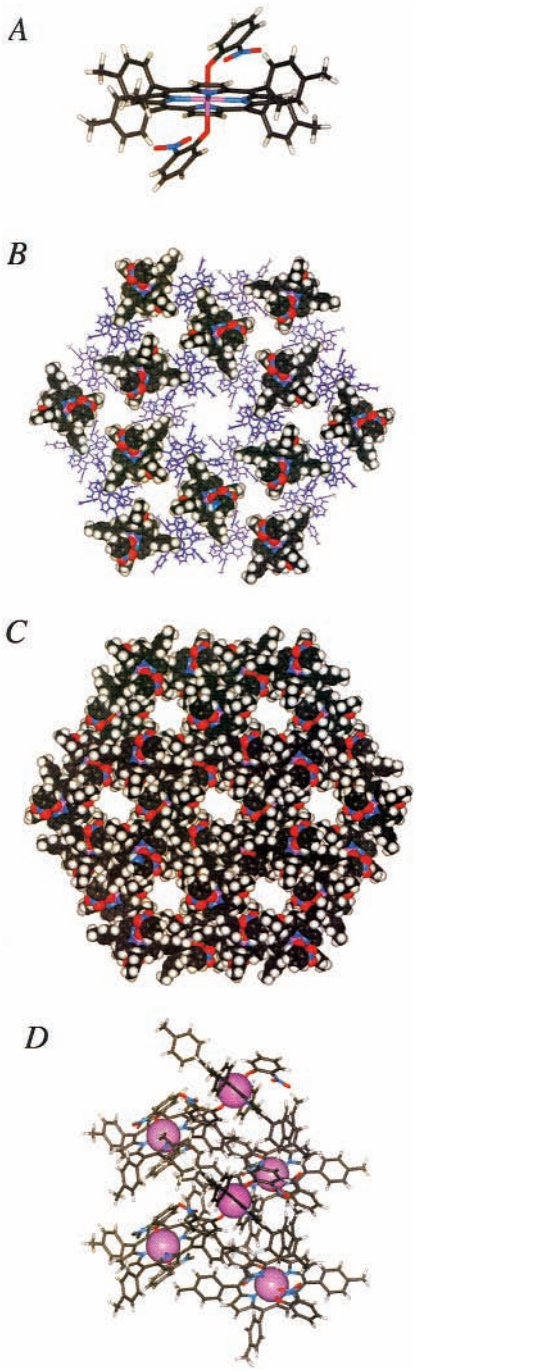

Figure 1. (A) A cylindrical bond representation of the molecular structure of the phenolate complex **1**. (B) The graphite-like arrangement found within one layer of the crystal structure of **1**. The Sn···Sn distance across the hexagonal is 36.68 Å. (C) A perspective view of the porous framework structure of an array of **1** down the crystallographic *c*-axis showing regular channels. (D) A view along the *ab* plane showing the helical nature of alternating voids between layers. The pink spheres represent tin(IV) atoms.

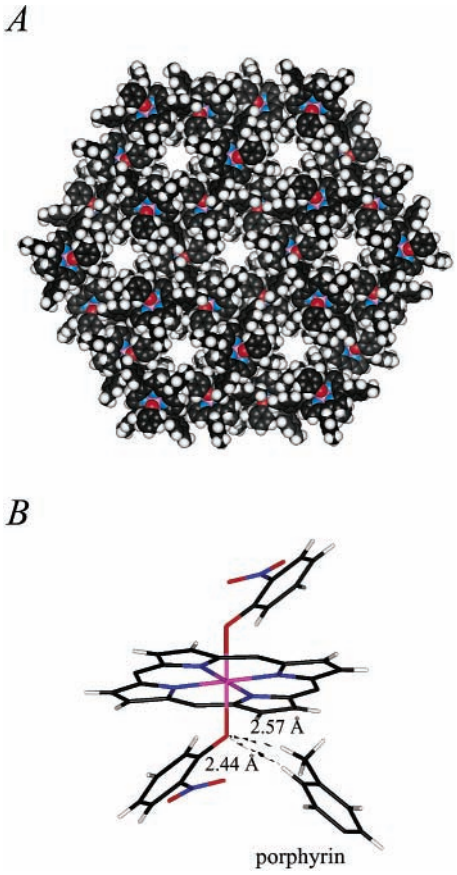

Figure 2. (A) The trigonal hexagonal unit cell of **2**. (B) An illustration of the weak nonclassical hydrogen bonding interactions between the tin(IV) oxygen of one porphyrin in one layer and two hydrogen atoms within the *meso*-tolyl group within another.

1D). Thus the arrays of **1** and **2** are made up of tight helical channels with pore diameters of 17 Å that pitch every 10 Å.

A view down the crystallographic *c*-axis shows that the metalloporphyrin arrays of **1** and **2** have an extremely open structure (Figures 1 and 2) dominated by a hydrophobic cavity of 5.5 Å diameter.[19] The porous structures exhibited by the arrays of **1** and **2** are a product of two events; the intersection of overlying voids within the helical channel resulting in a cylindrical-like channel and the extremely tight intermeshing of the *meso*-tolyl units between layers. In each case, the latter event is a result of weak but significant nonclassical hydrogen bonding interactions (C−H···O distances of 2.57 and 2.44 Å) between the tin(IV) oxygen of one porphyrin in one layer and two hydrogen atoms within the *meso*-tolyl group within another (Figure 2). The channels formed in crystals of **1** are lined with the axial aromatic nitro groups—a design feature indicating that these materials may become "active" with judicious choice of functionality replacement on the phenol. Although the intensity data were carefully measured at low temperature and corrected by analytical methods for absorption effects, the final difference electron density maps still contain very significant positive

(19) The potential generality of this self-assembly event is illustrated by a structure reported in ref 15. This report confirms the molecular structure of a tin(IV) phenolate by X-ray crystallography but overlooks the unique nature of the crystal packing—giving rise to the third example of porous materials prepared in this way. Again, the dimensions of the cavity so formed and the interactions with which it is formed are identical to **1** and **2**.

residual peaks of 1.6 and 1.1 e/Å^3. These peaks are significantly higher than the depth of the negative peaks and represent partly or fully disordered solvent species trapped within the crystal lattice.

TGA and DSC signals[20] associated with the analysis of crystals of **1** and **2** are shown in Figure 3. Endothermic

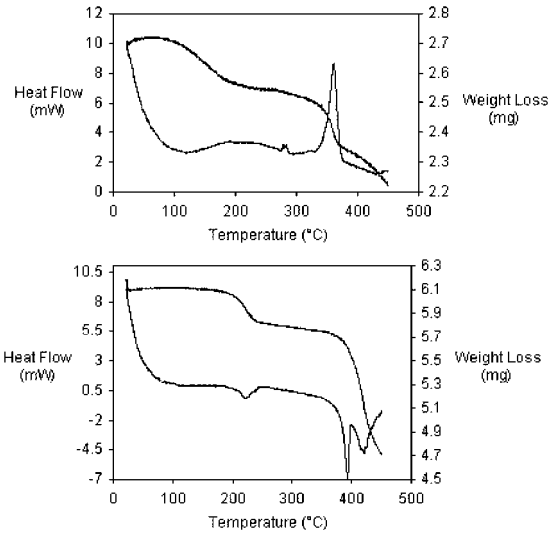

Figure 3. TGA and DSC results for crystals of **1** (top) and **2** (bottom).

processes at 95−220 °C for **1** (5−8% w/w loss) and at 180−250 °C for **2** (5−8% w/w loss) provide supportive evidence for the loss of included solvent from within the sieve-like materials. At higher temperatures however, the two materials behave quite differently. While the melting of **2** was evident at 390 °C, the degradation of **1** (with a resultant weight loss of 5−8% w/w) began at 290 °C. The difference seen the DSC and TGA between **1** and **2** at > 280 °C is most likely a result of the thermal loss of NO_x from **1** leading to the formation of a new and as yet unidentified material.

One of the underlying principles demonstrated by structures **1**, **2**, and **5**[15] involves the subtle cooperativity of weak intermolecular and crystal packing forces between different porphyrin phenolates that give rise to the sieve-like network. This cooperativity is selective enough to differentiate **1** and **5**[15] from **3**[10] and **4**,[14] which were crystallized under identical conditions without the generation of the same infinite channels (Table 1). Considering the difference in total size between the five porphyrin phenolates **1**−**5** is small, these results illustrate the power of molecular recognition at its most fundamental level.

Table 1. Crystal Structure Information for Porphyrin Phenolates **1**−**5** Illustrating the Subtly Associated with Channel Formation

compd	phenolate	space group	network
1	2-nitrophenoxy	*R*3bar	infinite channels
2	phenoxy	*R*3bar	infinite channels
3	4-nitrophenoxy	*P*21/n	no channels
4	2-naphthoxy	*P*1bar	no channels
5	1-naphthoxy	*R*3bar	infinite channels

The design and preparation of porous materials still provides a considerable challenge in materials chemistry, and as they stand, arrays of **1** and **2** fall short in rivalling zeolites, but they do provide a plausible approach to the construction of porphyrin-based networks. The basic approach is amenable to some variation (e.g., H for NO_2 or CH═CH−CH═CH) so it seems feasible that other appropriately designed systems may afford similar structures with variable porosity based on building block interactions. Investigations into further properties of these systems are in progress.

Acknowledgment. This work was supported in part by the Australian Research Council through the Special Research Centre for Green Chemistry and by the Special Monash University Research Fund (Nanochemistry). We wish to thank Prof. D. McFarlane and Dr. P. Newman for helpful discussions.

OL025935U

(20) Thermogravimetric analysis was performed in conjunction with differential scanning calorimetry using a STA1500 instrument. A sample of either **1** or **2** was placed in an aluminium pan under N_2 and data were collected between 30 and 450 °C with a temperature rate of 10 °C/min.